RECENT RESULTS FROM THE VEPP-2M COLLIDER AT NOVOSIBIRSK

E. P. Solodov

Budker Institute of Nuclear Physics, Novosibirsk, 630090, Russia

Representing the CMD-2 Collaboration*

ABSTRACT

The e^+e^- collider VEPP-2M at Novosibirsk is the only machine covering the energy range 360–1400 MeV. The peak luminosity is $\approx 5. \times 10^{30} cm^{-2} s^{-1}$ for the ϕ resonance region. Two modern detectors—the general-purpose magnetic detector CMD-2 and Spherical Neutral Detector (SND)—are taking data at the VEPP-2M collider.

The integrated luminosity about 10 pb^{-1} has been collected by both detectors. Latest results are presented in this paper.

1 VEPP-2M Collider

The VEPP-2M collider at the Budker Institute of Nuclear Physics in Novosibirsk, Russia, shown in Fig. 1, covers the center-of-mass energy range from the two pion threshold up to 1400 MeV (Ref. 1). Experiments at this collider yielded a number of important results in e^+e^- physics, including the most precise pion form factor measurements[2] and studies of the ϕ, ω, and ρ meson decays.[3,4] During 1988–1992, it was upgraded with a new booster to allow higher positron currents and injection of the electron and positron beams directly at the beam energy. After installation of the new booster, VEPP-2M has peak luminosity $L \approx 5.0 \times 10^{30} cm^{-2} s^{-1}$ at 40 mA per beam at the ϕ center-of-mass energy.

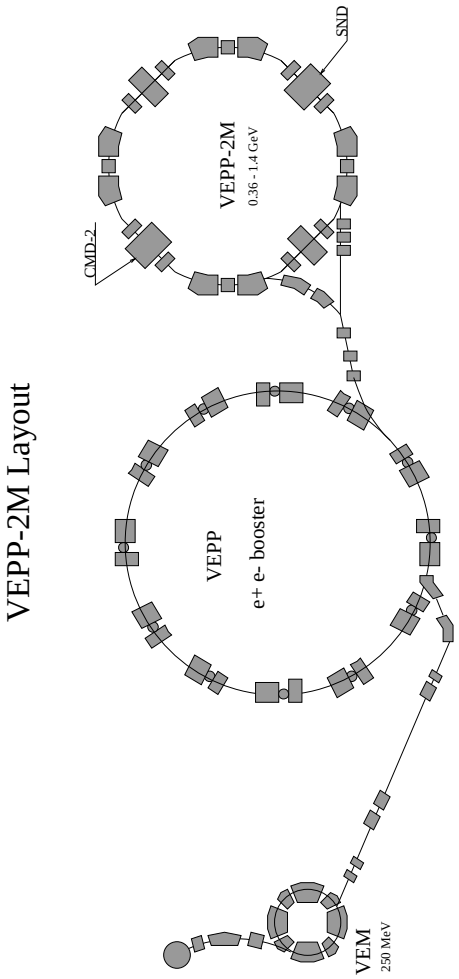

Figure 1: The layout of the VEPP-2M collider at the Budker Institute of Nuclear Physics in Novosibirsk.

2 The CMD-2 Detector

The CMD-2 detector has been described in more detail elsewhere.[5,6] The main systems of the detector are shown in Fig. 2.

The CsI barrel calorimeter with 6 x 6 x 15 cm^3 crystal size is placed outside a 0.4 r.l. superconducting solenoid with a 1 T azimuthally symmetric magnetic field. The endcap calorimeter is made of 2.5 x 2.5 x 15 cm^3 BGO crystals. The drift chamber inside the solenoid has about 250 μ resolution transverse to the beam and 0.5–0.6 cm longitudinally. The muon range system uses the streamer tubes and has 1–3 cm spatial resolution.

The collected sample of the Bhabha events was used for the calibration and determination of the reconstruction efficiency in the drift chamber and in the calorimeter. A momentum resolution of 5% for 500 MeV/c charged particles, and energy resolution of about 10% for gammas in the CsI calorimeter and about 8% in the BGO calorimeter have been obtained.

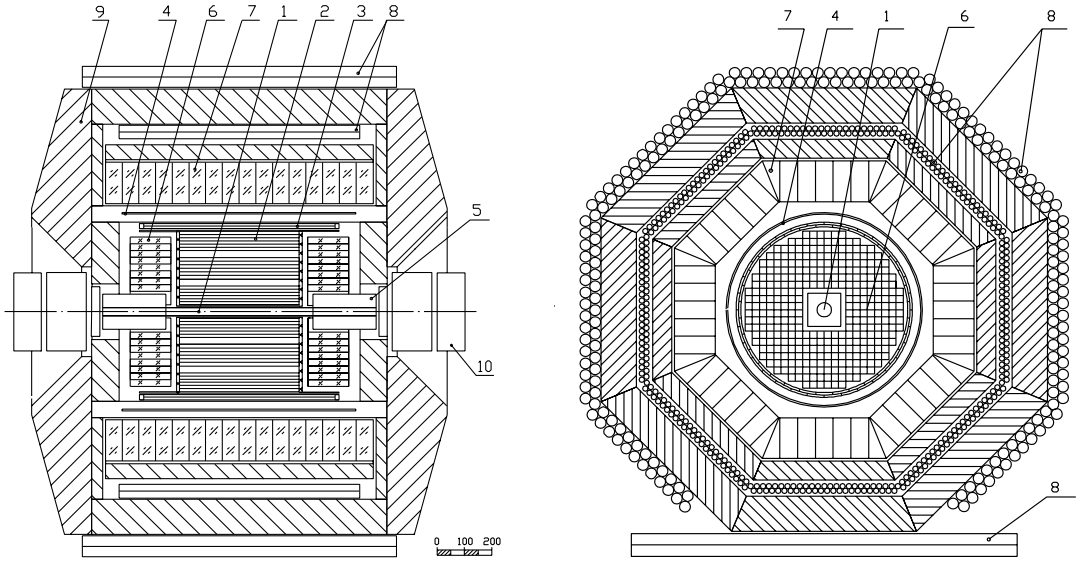

Figure 2: Horizontal and vertical cross sections of the CMD-2 detector. 1–vacuum chamber; 2–drift chamber; 3–Z chamber; 4–main solenoid; 5–compensating solenoid; 6–BGO end cap calorimeter; 7–CsI barrel calorimeter; 8–muon range system; 9–magnet yoke; 10–collider lenses.

The data with the luminosity integral $\approx 300\ nb^{-1}$ collected in 1992–1993 at ϕ

were used for the measurement of ϕ meson parameters and branching ratios into four major decay modes.[7]

The integrated luminosity $\approx$ 1500 nb^{-1} around ϕ mass has been collected during the 1993 summer run and was used for studies of rare decay modes of ϕ, coupled $K_S K_L$ decays, and nuclear interactions of neutral kaons. Some preliminary results are published in Ref.,[8] and in this paper, we present the latest analysis based on 1992–1993 data.

The 1994–1995 runs were dedicated mostly to measurements of the total hadronic cross section at the energies below ϕ resonance[9] where the integrated luminosity about 500 nb^{-1} has been collected. In this paper, we present preliminary results on ω meson parameter measurements based on 122 nb^{-1} collected around ω peak.

An additional 2000 nb^{-1} have been collected around ϕ peak in the 1996 spring run, and these data are under analysis now.

2.1 Rare ϕ Decays Study

2.1.1 $\phi \to \eta\gamma$ and $\phi \to \eta'\gamma$

The decay $\phi \to \eta\gamma$ was previously observed in neutral modes ($\eta \to \gamma\gamma,\ \eta \to 3\pi^0$) only. The detector CMD–2 gives the possibility to study $\phi \to \eta\gamma$ decay in the channel with charged particles, when η decays into $\pi^+\pi^-\pi^0$. The primary photon has the highest energy of all three in the final state - 362 MeV at the ϕ meson peak and was required be detected in events selection.

The reconstructed invariant mass of three pions, $M_{\pi^+\pi^-\pi^0}$, was used to select the decay $\phi \to \eta\gamma$, and the distribution over it had a peak around $M_\eta = 547.45$ MeV. After background subtraction, 1100±40 events were selected.

The experimental cross section $\sigma(e^+e^- \to \phi \to \eta\gamma)$ with a fit function is presented in Fig. 3. The obtained parameters of ϕ meson M_ϕ=1019.31±0.18 MeV and Γ_ϕ=4.70±0.25 MeV are in good agreement with table values.[10] Using the electron width of ϕ from Ref.,[10] the $Br(\phi \to \eta\gamma)$ was found to be:

$$Br(\phi \to \eta\gamma) = (1.29 \pm 0.07) \times 10^{-2}.$$

The decay $\phi \to \eta'\gamma$ was searched in the mode, when η' decays into $\pi^+\pi^-\eta$ and $\eta \to \gamma\gamma$. So, both $\eta\gamma$ and $\eta'\gamma$ final states have two charged particles and three

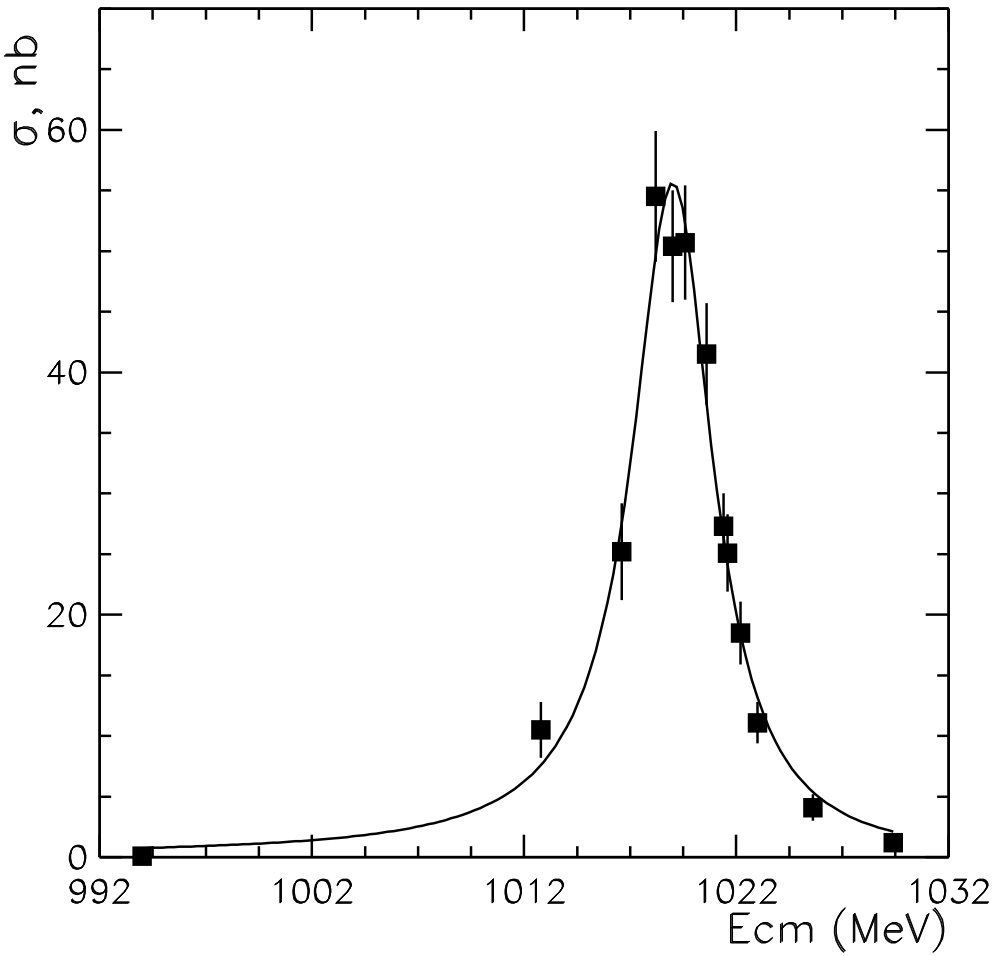

Figure 3: The $\phi \to \eta\gamma$ cross section.

photons. The events with all these particles detected were used for the constrained fit, and as a result, 481 events of $\eta\gamma$ were selected.

The decay into $\eta\gamma$ is the basic background for the $\eta'\gamma$ search, and after the anti–$\eta\gamma$ cut, the scatter plot of the invariant mass of the two hardest photons M_{12} versus the weakest photon energy ω_3 was studied. For $\eta'\gamma$ events, M_{12} should be close to η mass 547.5 MeV, while ω_3 is a monochromatic 60 MeV photon. Figure 4 presents the result of 1992–1993 data together with a simulation of $\phi \to \eta'\gamma$. We have one candidate to $\eta'\gamma$ event with one event as estimated background. Using for the 90% C.L. upper limit $N_{\eta'\gamma}$ <3 and the efficiencies obtained from the simulation, $\varepsilon_{\eta\gamma} = 14.4\%$ and $\varepsilon_{\eta'\gamma} = 6.4\%$, the following result has been obtained:

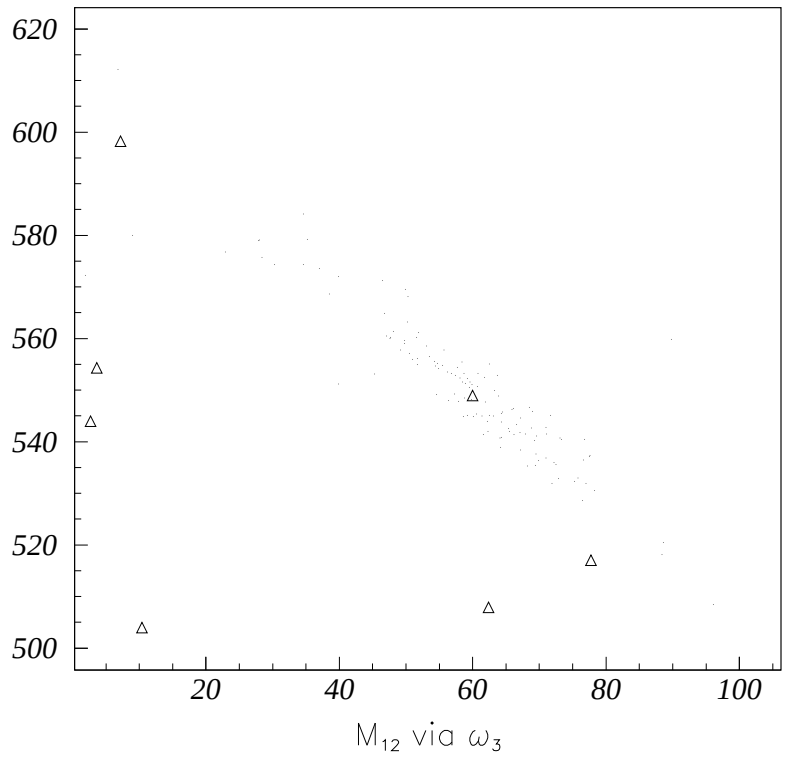

Figure 4: Invariant mass M_{12} (MeV) vs. ω_3 (MeV) after constrained fit. Dots are simulations, and triangles are experiment.

$$Br(\phi \to \eta'\gamma) \; < \; 2.4 \cdot 10^{-4}.$$

2.1.2 Search for $\phi \to \pi^+\pi^-\pi^+\pi^-$

Three- and four-track events were selected as candidates for the process $\phi \to \pi^+\pi^-\pi^+\pi^-$. But due to a high background from the main channels of ϕ decaying into three-track events, in the search for the process $\phi \to \pi^+\pi^-\pi^+\pi^-$, only four-track events were used. The ratio of three- and four-track events at the energy points outside the ϕ meson region was used (along with a simulation) for evaluation of a detection efficiency.

To extract the number of events of the process $e^+e^- \to \pi^+\pi^-\pi^+\pi^-$, we apply a simple cut to the total momentum of four charged particles (should be around zero) and their total energy (should be around $E_{c.m.}$ energy), assuming that all particles are pions.

The cross section vs. energy for the process $e^+e^- \to \pi^+\pi^-\pi^+\pi^-$ is shown in Fig. 5. Only statistical errors are shown. A function which describes interference of linear background with the amplitude of the process $\phi \to \pi^+\pi^-\pi^+\pi^-$ was used

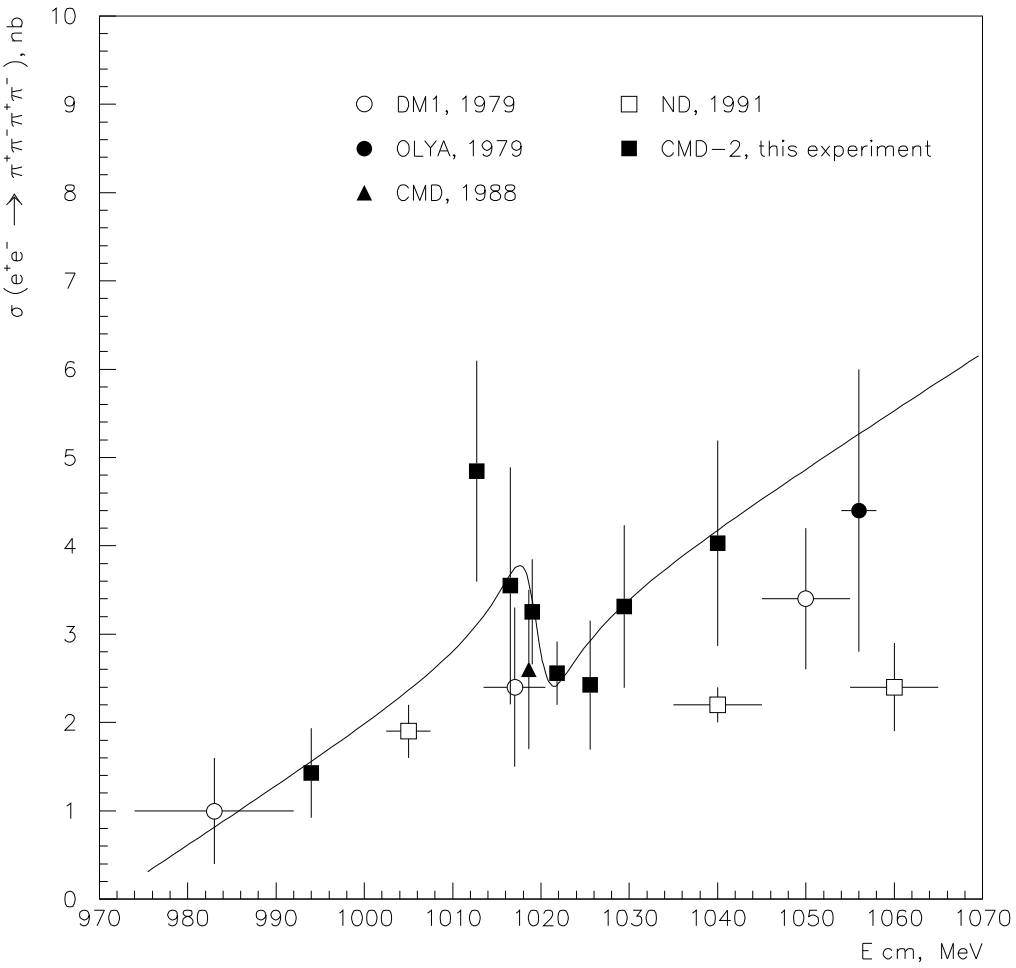

Figure 5: The cross section $e^+e^- \to \pi^+\pi^-\pi^+\pi^-$.

for the fitting taking into account only this experiment. The result of the fit is shown in the plot by a smooth line. Using this fit and the uncertainty in the efficiency, one can get

$$Br(\phi \to \pi^+\pi^-\pi^+\pi^-) < 1. \times 10^{-4},\ 90\%\ \text{C.L.}$$

2.1.3 Search for $\phi \to f_0(980)\gamma$

The event candidates were selected by a requirement of two charged tracks in the DC and one or two photons with energy greater than 20 MeV in the CsI calorimeter. All particles were required to be in the polar angle between 0.85 and 2.25 radians for the bremsstrahlung processes suppression. The sum of the energy

depositions of two clusters associated with the charged tracks was required to be less than 450 MeV to remove Bhabha events.

The main background for the studied process was $\phi \to \pi^+\pi^-\pi^0$ decay when one of the gammas from π^0 escaped detection. To reduce this background, a constrained fit was used. The rest of the 3π background was removed by selection of gamma energy in the range 20 MeV$< E_\gamma <$100 MeV, where signal of f_0 was expected. The muon range system was used to remove $\mu^+\mu^-\gamma$ contamination.

Under these conditions, 833±30 events of $\pi^+\pi^-\gamma$ and 846±31 of $\mu^+\mu^-\gamma$ events were selected with the integrated luminosity of 1269 nb^{-1}, determined by Bhabha events. The detection efficiency was found by simulation to be 17%. The experimental cross sections vs. center-of-mass energies are presented in Figs. 6(a) and (b).

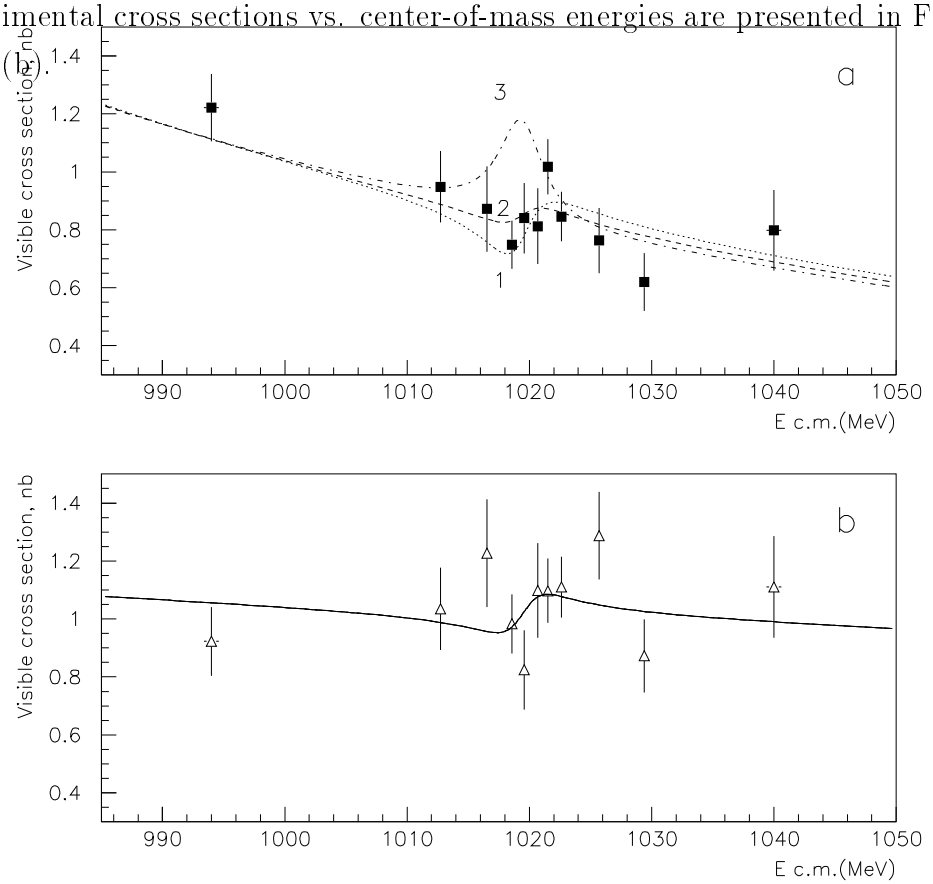

Figure 6: (a) Visible cross section for $e^+e^- \to \pi^+\pi^-\gamma$. Lines are theoretical predictions in case of no $f_0\gamma$ signal (2), $f_0\gamma$ signal with B$(\phi \to f_0\gamma) = 2.4 \times 10^{-4}$ for negative relative phase (3), and positive relative phase (1). (b) Visible cross section for $e^+e^- \to \mu^+\mu^-\gamma$ with theoretical prediction.

The signal from $\phi \to f_0(980)\gamma$ decay was searched as interference patterns

in the cross section vs. energy behavior of the $e^+e^- \to \pi^+\pi^-\gamma$ process and in the difference in gamma spectra of the selected events at ϕ peak and near the ϕ region. According to the theoretical calculations,[11] the following interference patterns were used for $f_0\gamma$ search: (a) interference of the background process $e^+e^- \to \pi^+\pi^-\gamma$ with "radiative" decay of $e^+e^- \to \phi \to \gamma \to \pi^+\pi^-\gamma$ when no f_0 is present. This is valid also for the $\mu^+\mu^-\gamma$ process; and (b) interference of the two above processes with $e^+e^- \to \phi \to f_0\gamma \to \pi^+\pi^-\gamma$ when f_0 was described as a four-quark state. The model predictions are shown in Figs. 6(a) and (b) for the cross section and in Fig. 7 for the difference in gamma spectra.

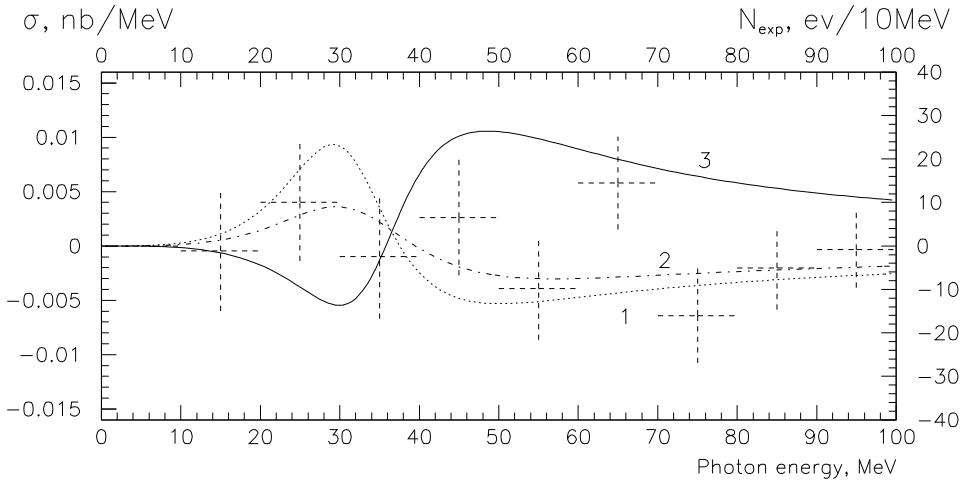

Figure 7: Difference in spectrum for gamma at "ϕ" region and "non-ϕ" region, normalized to integrated luminosity. Lines are theoretical prediction for the four quark model for the 2.4×10^{-4} branching ratio in case of positive (1) and negative (3) interference signs with 40 MeV f_0 width. Line (2) is for 100 MeV f_0 width.

Using these interference patterns, the following results were obtaind at the 90% C.L.:
$Br(\phi \to \pi^+\pi^-\gamma) < 1.5 \times 10^{-5}$,
$Br(\phi \to \mu^+\mu^-\gamma) < 2.6 \times 10^{-5}$,
$Br(\phi \to f_0\gamma) < 7 \times 10^{-4}$.

2.1.4 Search for $\phi \to \eta e^+e^-$

The decay mode $\eta \to \gamma\gamma$ was chosen. The typical characteristics are the invariant mass of the two gammas (0.54 GeV), the small space angle between the two electrons, and the sum of the momenta of the electrons (0.364 GeV). The main backgrounds are: (a) $\phi \to \eta\gamma$ with gamma conversion in the beam pipe and (b) $e^+e^- \to e^+e^-\gamma\gamma$ where the two electrons come from an internal gamma conversion. Full kinematical reconstruction was done and calibrated with $\phi \to \pi^+\pi^-\pi^0$ events at a small angle between the two charged pions. The QED process $e^+e^- \to e^+e^-\gamma$ was used to calibrate efficiency of the drift chamber for charged particles at small space angle and photon conversion probability in the beam pipe. The total luminosity was 2085 nb^{-1}, corresponding to 2,715,000 ϕ's.

In the region indicated in Fig. 8 around η mass 12 events are seen and 4.2 are expected from all backgrounds. The branching ratio was found to be

$$Br(\phi \to \eta e^+e^-) = (1.10\pm\ 0.49\pm0.19)\times10^{-4}.$$

2.2 Measurements of ω Meson Parameters

The c.m. energy region from 2 x 380 to 2 x 405 MeV has been scanned at 13 energy points with a total luminosity integral of 122 nb^{-1}. The beam energy in each point has been measured by the resonant depolarization technique[12] and is known to an accuracy better than 10^{-4}.

Events with two noncollinear tracks were selected as a candidate for a $\omega \to \pi^+\pi^-\pi^0$ decay. The resulting number 13489 of $\pi^+\pi^-\pi^0$ events was obtained by fitting the missing mass $M^2_{\pi^0}$ parameter histograms and background subtraction.

Events with two detected gammas from neutral pions were used for the combined trigger and reconstruction efficiency determination, which was found to be 0.91 ± 0.01.

Luminosity was determined by the number of the Bhabha events, selected by the presence of two collinear tracks in the Drift Chamber and high energy deposition in the CsI barrel calorimeter with the statistical error in each energy point on the level of 1–2 %.

Experimental points together with the fitted excitation curve are shown in Fig. 9.

The following ω-meson parameters were obtained from the fit:

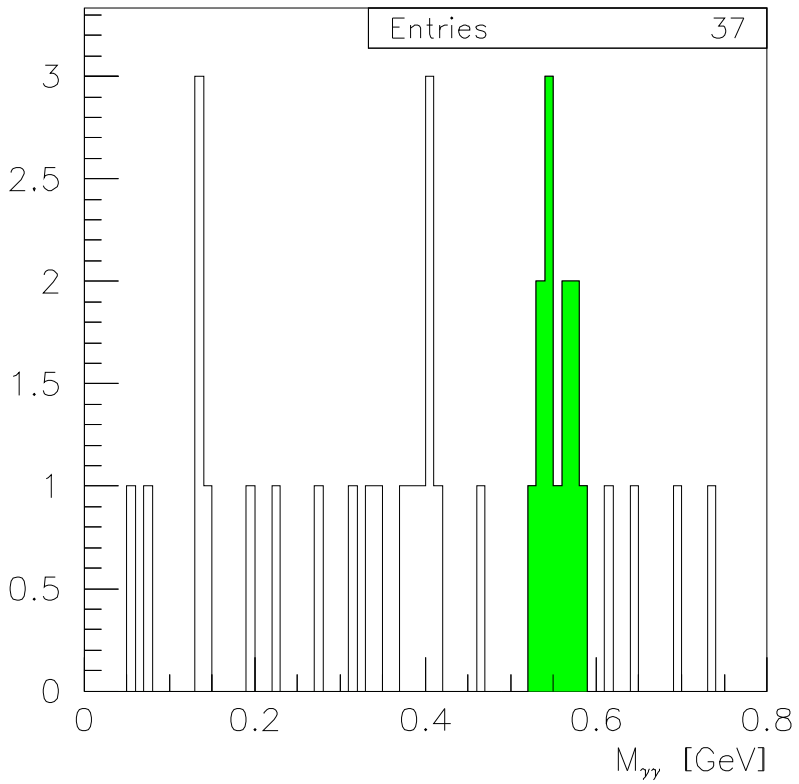

Figure 8: The invariant mass of the two photons after constraind fit.

$\Gamma_{e^+e^-} = 0.62 \pm 0.01 \pm 0.02$ keV,
$\Gamma_{tot} = 8.23 \pm 0.20 \pm 0.30$ MeV.

2.3 $K_S K_L$ Couple Decays and Interaction Study

As it was realized at the very early steps of the ϕ meson studies at the colliding beam machines, $K_S K_L$ pairs can be used for studying CP and CPT violation. These suggestions, including studies of quantum mechanical correlations, were discussed in Refs.[13,5] for experiments at VEPP-2M (Ref.[1]), an electron-positron collider at the Budker Institute of Nuclear Physics in Novosibirsk, Russia, and carefully reviewed by Ref..[14]

The ϕ resonance produced in e^+e^- collisions can also be considered as a source of the η,η' mesons[15] and the low momentum neutral and charged kaon pairs for

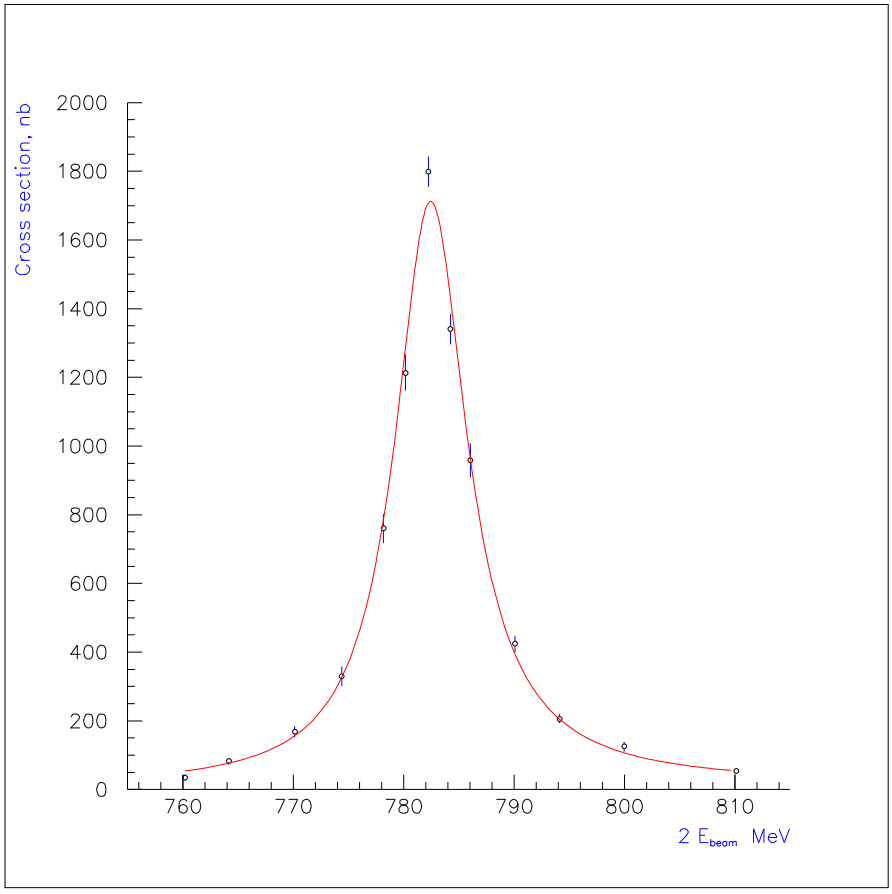

Figure 9: ω meson excitation curve.

studies of nuclear interactions.

The construction of the ϕ factories in Novosibirsk and Frascati[16,17] will make feasible new precise measurements of a possible direct component in the decay $K_L \to \pi^+\pi^-, \pi^0\pi^0$ (ϵ'/ϵ).

At the VEPP-2M collider with the peak luminosity $L \approx 5. \times 10^{30} cm^{-2}s^{-1}$ which could be considered as a pre-ϕ factory with the CMD-2 detector, some useful measurements can be done to prepare for running at the ϕ factories. An upgrade of the collider to $10^{32} cm^{-2}s^{-1}$ luminosity has been planned for investigating the idea of the round beams, an important ingredient of the Novosibirsk ϕ-factory project.[18] A 3.4 cm diameter vacuum beam pipe inside the CMD-2 detector is made of Be with a 0.077 cm wall thickness and may be considered as a target for studies of the kaon nuclear interaction.

2.3.1 Selection of $K_S K_L$ Coupled Decays

Candidates were selected from a sample in which two vertices, each with two opposite charge tracks, were observed within 15 cm from the beam axes and all tracks were reconstructed. An example of such an event is shown in Fig. 10.

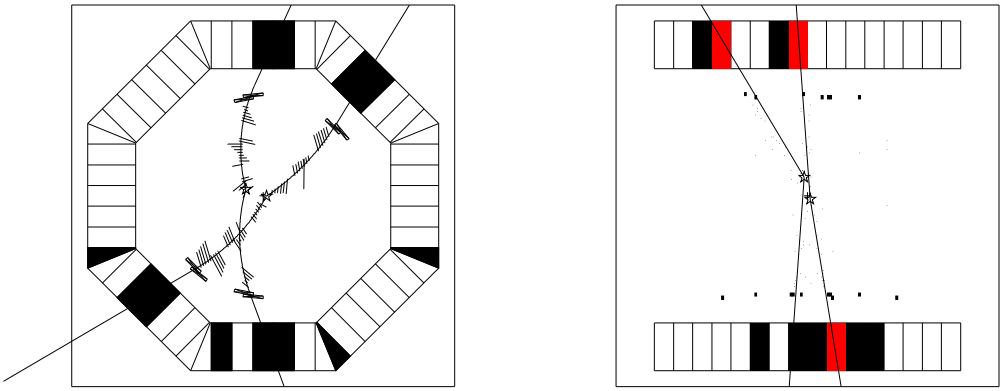

Figure 10: $\phi \to K_S K_L$ event with coupled decay.

The cuts $470 MeV/c^2 < M_{inv} < 525 MeV/c^2$ and $80 MeV/c < P_{mis} < 140 MeV/c$, with an additional requirement to have another reconstructed vertex in the P_{mis} direction, select $K_S \to \pi^+\pi^-$ events in one of the vertices. In this case, K_L is expected to be in the other one.

Figure 11(a) shows the decay length distribution for selected K_S's with the correct 0.55±0.02 cm decay length. The decay radius distribution for the K_L's with two charged tracks in final state is shown in Figure 11(b). At the flat region, where reconstruction efficiency is uniform, a peak is seen at the radius of 1.7 cm corresponding to the 79 ± 18 of K_L's which interacted with nuclei in the Be tube. The remaining 1355 events are representing K_L decaying in flight.

To select candidates to $K_L \to \pi^+\pi^-$ events additional cut requiring the invariant mass of two tracks from a K_L vertex to be in the range of 470–525 MeV/c^2 was applied. The obtained distribution is presented in Fig. 11(d) together with the fit function where all parameters except the number of events are fixed at the values obtained from the distribution in Fig. 11(b). The number of events under the peak drops down to 31 ± 7 and 78 remain from K_L decays in flight. One can apply stronger requirements for these events to satisfy $K_L \to \pi^+\pi^-$ kinematics within detector resolution, i.e., $80 MeV/c < P_{mis} < 140 MeV/c$ and K_S vertex in the P_{mis} direction. This selection is illustrated in Fig. 11(d) by the shaded histogram. The peak at the Be tube survives with 20±5 events and 35 K_L decays in flight remain.

The 28.5 ± 6.4 events found in the peak after the invariant mass cut and some efficiency corrections are interpreted as regeneration of K_L into K_S with its decay into $\pi^+\pi^-$, and another 50 ± 17 peak events represent nuclear interactions with

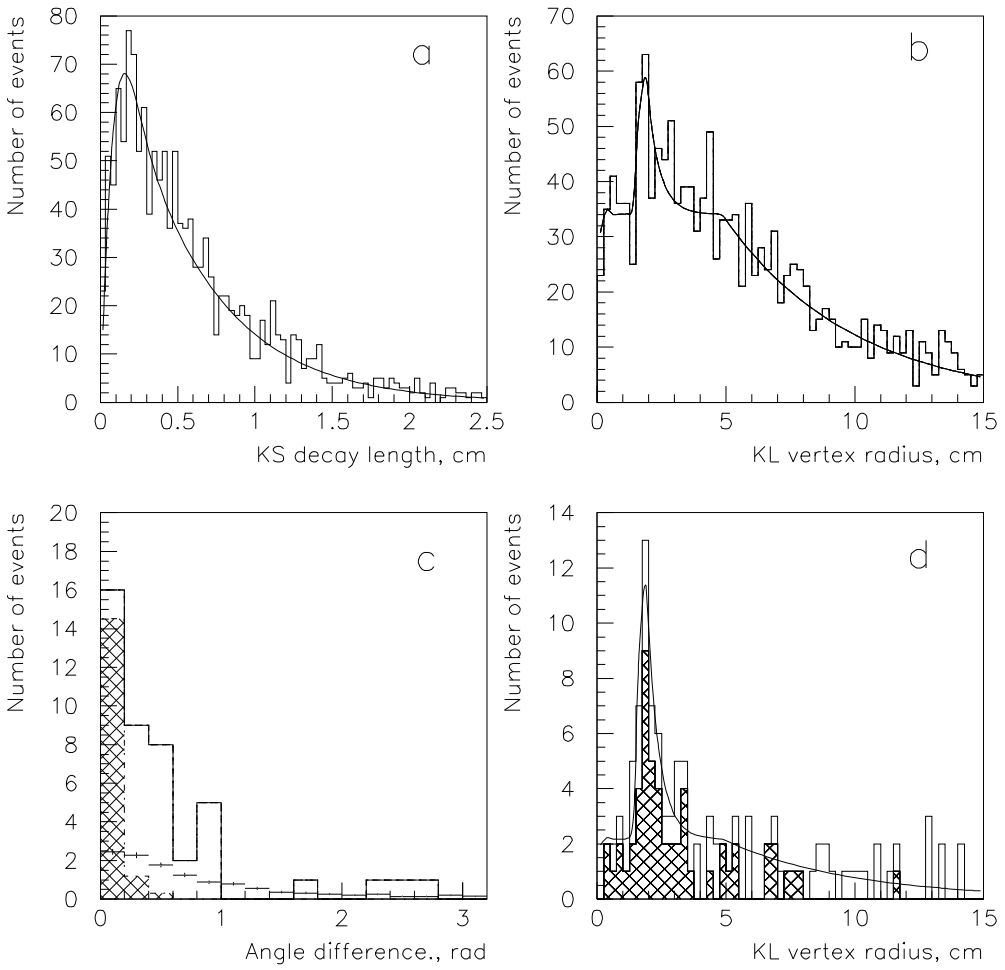

Figure 11: (a) Decay length for K_S. (b) Decay radius for K_L. (c) Projected angular distribution for "tube" events (histogram), K_L semileptonic decays (points with errors), and K_S two-pion decays (shaded). (d) Decay radius for K_Ls after M_{inv} cut and after K_S selecting cut (shaded).

two visible charged particles.

Using simulated efficiencies for estimation of the full number of K_L passed the berillium pipe, the following cross sections for regeneration and visible inelastic scattering have been obtained:
$\sigma_{reg}^{Be} = 58 \pm 17$ mb.
$\sigma_{inel}^{vis} = 77 \pm 26$ mb.

The sources of the inelastic scattering events are the reactions with Σ and Λ production. To estimate the total cross section, the relative weight of these reactions was taken 0.21 from the CERN GEANT code (NUCRIN). With the

ratio $\sigma_{inel}/\sigma_{tot} = 0.52$,[19] one can estimate $\sigma_{tot}^{Be} = 705 \pm 238$ mb.

A histogram in Fig. 11(c) shows the projected angular distribution for the regenerated at the beam pipe K_S along with the background from the semileptonic decays of K_L (dots with errors). The obtained angular distribution is wider than in the case of coherent regeneration, which can be illustrated by the shown shaded distribution for original K_S decays at the same distance. But with the available sample, coherent contamination cannot be extracted.

2.3.2 Discussion

The selection of candidates for $K_L \to \pi^+\pi^-$ events faced two problems. First was a background from the dominant semileptonic K_L decays which already was discussed in Ref.[20] and seemed to be solvable with better DC resolution.

A second problem was relatively high background from nuclear interactions of K_L and the regeneration effect which was for the first time experimentally observed for slow kaons.

In Fig. 12(a), the experimental regeneration cross section is plotted together with the theoretical calculations for Be and Cu performed in Ref..[19] The comparison of the calculated regeneration cross sections for these two different materials shows that at momenta below 200 MeV/c, one cannot scale them by a simple $A^{2/3}$ dependence. The experimental angular distribution of the regenerated K_S after

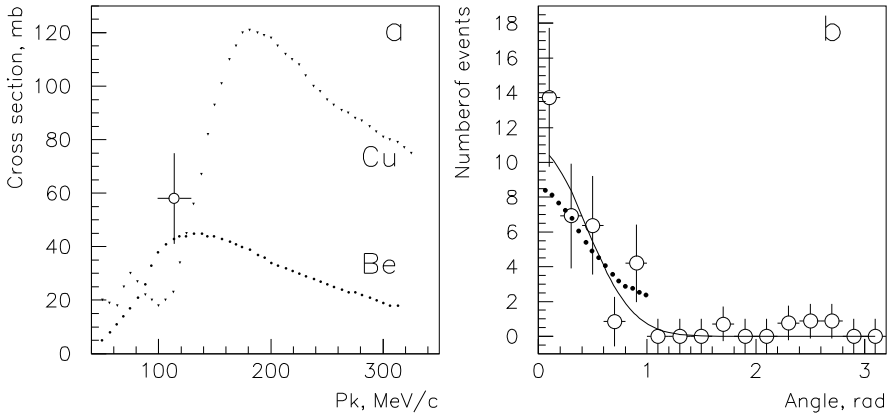

Figure 12: (a) Experimental regeneration cross section and theoretical calculations for Be and Cu. (b) Projected angular distribution of the regenerated K_S with fit function (solid line) and theoretical prediction (dots).

background subtraction is presented in Fig. 12(b) together with the fit function and theoretical prediction,[19] and seems to be more narrow.

The obtained experimental value of the total nuclear cross section in Be for 110 MeV/c kaons is shown in Fig. 13 together with the experimental data at higher momenta[21] and theoretical calculations.[19] The cross sections extracted from the GHEISHA and FLUKA simulation codes are also shown. It is seen that the FLUKA code, as well as the calculations from Ref.,[19] are in good agreement with experimental data. The GHEISHA code gives completely wrong absolute values as well as momentum dependence.

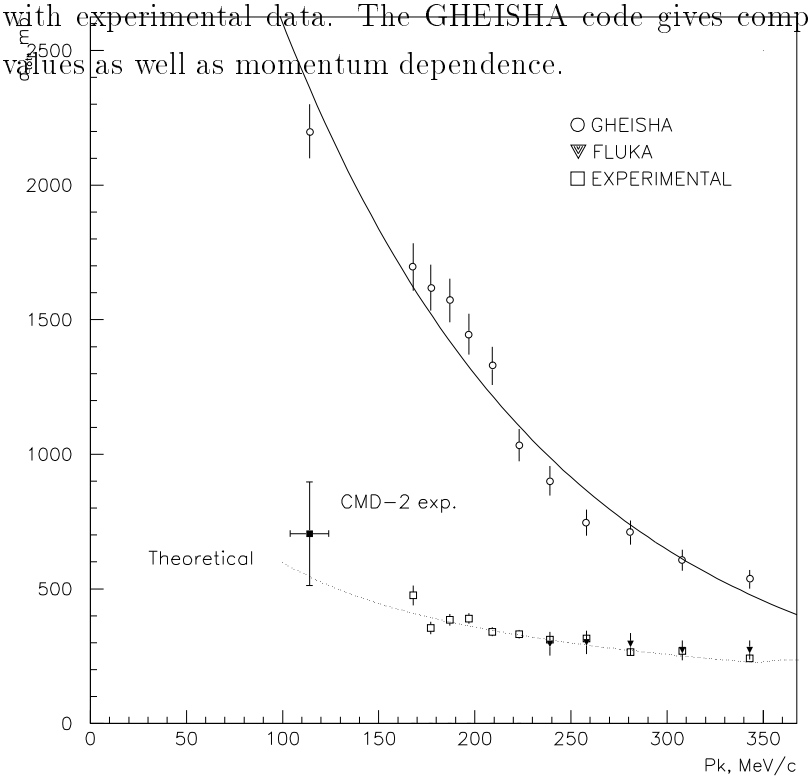

Figure 13: Comparison of the total experimental K_L nuclear interaction cross section in Be with the theoretical calculations and simulation by different codes.

After publishing our preliminary results,[8] the regeneration influence was discussed for the ϵ'/ϵ measurement planned in the KLOE detector.[19] It was shown that the total regeneration probability in the KLOE drift chamber after an acoplanarity cut (factor of four rejection) was 10^{-4} that should be compared with 2×10^{-3} probability for the "normal" CP-violating $K_L \to \pi\pi$ decay and $\approx 10^{-6}$ probability for the direct CP-violation decay.

The regeneration itself does not give any decay asymmetry expected for the direct CP-violating K_L decay, but the acoplanarity cut as well as another selection cut applied separately to $\pi^+\pi^-$ and $\pi^0\pi^0$ final states with a different resolution (DC for the first and calorimeter for the second) can cause systematic asymmetry

due to the broad angular distribution of the regenerated events.

2.4 Search for $\eta \to \pi^+\pi^-$ Decay

As it was mentioned before, the radiative $\phi \to \eta\gamma$ decay can be considered as a source of η mesons, accompanied with 362 MeV energy gamma.

With analyzed luminosity integrals, 28056 η's were produced. The selected $\pi^+\pi^-\gamma$ events (see above) can be used to search for CP-violation decay $\eta \to \pi^+\pi^-$. This decay can be seen as a peak in the photon-energy histogram at the 362 MeV region. Figure 14 shows photon-energy distribution after constrained fit and some additional cuts to reduce $\phi \to 3\pi$ background. Shaded histograms show simulated signals from $\eta \to \pi^+\pi^-$ decays before and after constrained fit. The detection efficiency for these events was found by simulation to be $9.9 \pm 0.9\%$. No signal was seen in the experimental distribution, and the upper limit was found to be:

$$\mathrm{B}(\eta \to \pi^+\pi^-) \ < \ 2.1 \times 10^{-3}.$$

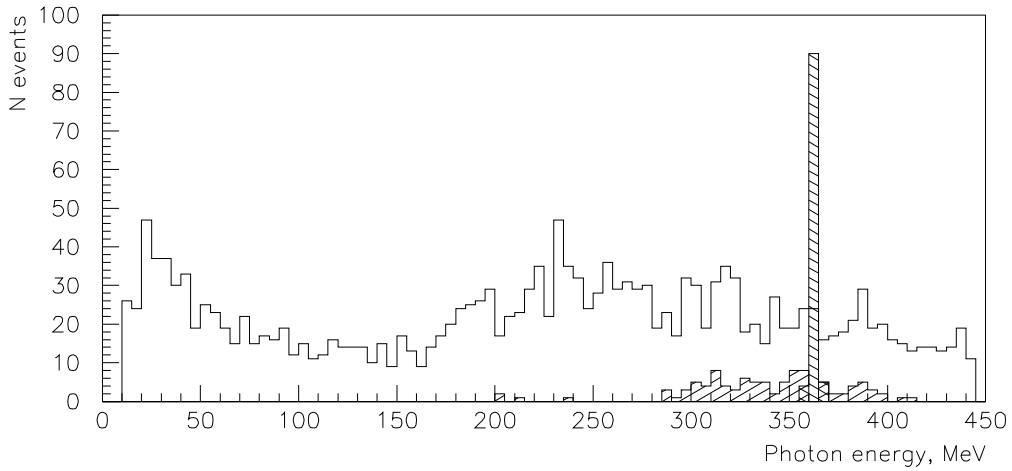

Figure 14: Photon energy for $\phi \to \pi^+\pi^-\gamma$ events to search for $\eta \to \pi^+\pi^-$ decay. Simulated signals before and after constrained fit are shown shaded.

2.5 CMD-2 Results Summary

The CMD-2 detector is taking data at the VEPP-2M collider in Novosibirsk. Data collection was performed at the ϕ meson region and at the energy range 600–1000

MeV. About 30% of the available data have been analyzed. The new results in rare ϕ decays study
$Br(\phi \to \eta\gamma) = (1.29 \pm 0.07) \times 10^{-2}$,
$Br(\phi \to \eta\prime\gamma) < 2.4 \times 10^{-4}$,
$Br(\phi \to \pi^+\pi^-\pi^+\pi^-) < 1.0 \times 10^{-4}$,
$Br(\phi \to f_0\gamma) < 7 \times 10^{-4}$,
$Br(\phi \to \pi^+\pi^-\gamma) < 1.5 \times 10^{-5}$,
$Br(\phi \to \mu^+\mu^-\gamma) < 2.6 \times 10^{-5}$,
$Br(\phi \to \eta e^+e^-) = (1.10 \pm 0.49 \pm 0.19) \times 10^{-4}$
have been obtained.

A search of CP-violation decay $\eta \to \pi^+\pi^-$ based on about 23000 of η gives an upper limit $\mathrm{B}(\eta \to \pi^+\pi^-) < 2.1 \times 10^{-3}$.

With the CMD-2 detector, the coupled K_SK_L decays have been observed for the first time.

The measured values of the cross sections indicate that regeneration will cause an additional background for the CP-violating decays of K_L at the ϕ-factory experiments and should be carefully studied to avoid systematic errors.

Acknowledgments

The authors would like to thank R. Baldini and A. Michetti for useful discussions on the nuclear interaction studies and cooperation in this field.

This work is supported in part by the U.S. Department of Energy, U.S. National Science Foundation, and the International Science Foundation under grants RPT000 and RPT300.

3 Spherical Neutral Detector

3.1 Introduction

After installation in 1995, the experiments with the new SND detector at the e^+e^- collider VEPP-2M were continued. SND is a general-purpose nonmagnetic detector with a spherical NaI(Tl) calorimeter. Its parameters, like energy and spatial resolution, background, recording rate, etc., obtained during the run in the energy range around $\phi(1020)$, and some preliminary results on $\phi(1020)$ decays, showing detector performance, are presented.

3.2 SND Detector Overview

SND[22] is a general-purpose nonmagnetic detector, consisting of the tracking system, three spherical layers of NaI(Tl) crystals, and an outer system of streamer tubes and plastic scintillation counters (Fig. 15).

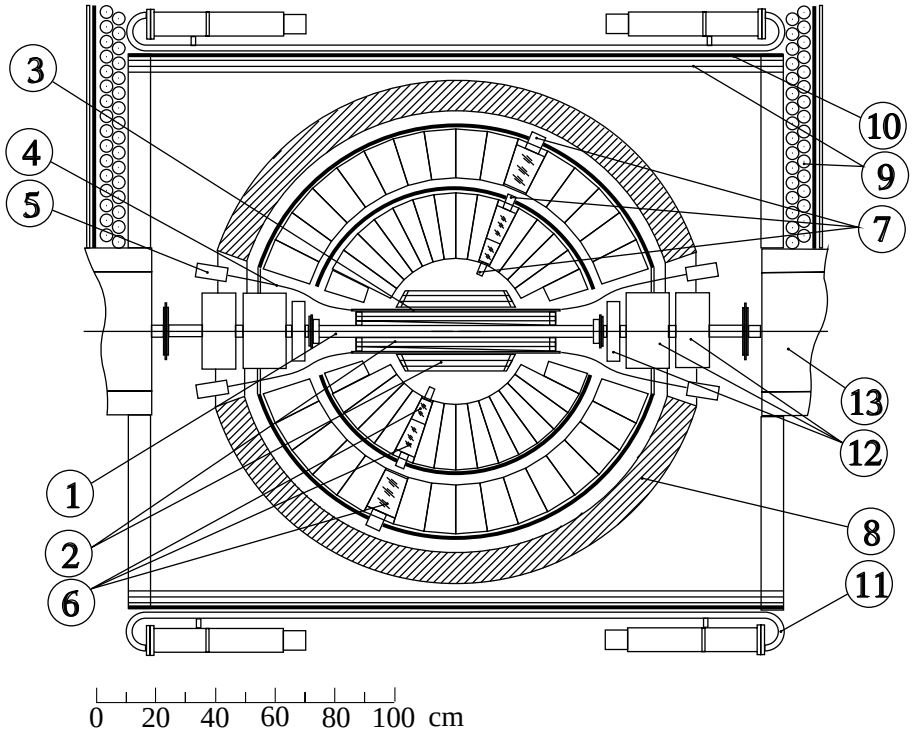

Figure 15: Detector SND—view transverse to the beam. 1—beam pipe, 2—drift chambers, 3—scintillation counters, 4—fiber lightguides, 5—PMT's, 6—NaI(Tl) counters, 7—vacuum phototriodes, 8—iron absorber, 9—streamer tubes, 10—1 cm iron plates, 11—scintillation counters, 12—magnetic lenses, 13—bending magnets.

The NaI(Tl) calorimeter consists of 1632 individual crystals of 3.6 tons total weight. The calorimeter thickness in the radial direction is 35 cm $\sim$ 13.5 X_0. The angular size of each crystal is $\Delta\phi = \Delta\theta = 9^o$; the solid angle coverage of the calorimeter is 90% of 4π. Each crystal is viewed by a vacuum phototriode[23] with a charge-sensitive preamplifier, located on the crystal. The calorimeter calibration procedure is based on the use of cosmic muons.[24]

The tracking system consists of two cylindrical drift chambers. Both chambers are divided into 20 jet-type cells in the azimuthal plane. Each cell contains five

sensitive wires. The longitudinal coordinate is measured by the charge division method with the accuracy of 3 mm. In addition, cathode strip readout for inner and outer layers provides the improvement of the latter value to 0.5 mm.

The muon/veto system consists of plastic scintillator counters and streamer tubes.

3.3 The Physical Program at VEPP-2M

The physical program for SND includes the following processes:

- Radiative decays of $\rho, \omega, \phi \to \pi^0\gamma, \eta\gamma$; $\phi \to \eta'\gamma$; $\phi \to a_0\gamma, f_0\gamma, \pi\pi\gamma, \eta\pi\gamma$; $\rho, \omega \to \pi\pi\gamma$.
- OZI and G-parity suppressed decays $\phi \to \omega\pi, \pi\pi, \eta\pi\pi$; $\rho \to 3\pi$; $\omega \to 2\pi$.
- Electromagnetic decays $\rho, \omega, \phi \to \eta e^+e^-, \pi^0 e^+e^-$.
- e^+e^- annihilation into hadrons $e^+e^- \to 2\pi, 3\pi, 4\pi, 5\pi$; $e^+e^- \to \omega\pi, \eta\pi\pi, \phi\pi$; $e^+e^- \to K^+K^-, K_SK_L, KK\pi$.
- Test of QED $e^+e^- \to 3\gamma, e^+e^-\gamma$ $(2 \to 3)$; $e^+e^- \to 4\gamma, e^+e^-\gamma\gamma, 4e$ $(2 \to 4)$; $e^+e^- \to 5\gamma, 3\gamma e^+e^-, 4e\gamma$ $(2 \to 5)$.
- Search for rare K_S decays $K_S \to 2\gamma, 3\pi^0, 2\pi^0\gamma, \pi^0\gamma\gamma, \pi^0 e^+e^-$
- Search for rare η decays $\eta \to 3\gamma, e^+e^-, 4e, 2\pi^0$.
- Search for C-even reactions $e^+e^- \to \eta', a_0, f_0, a_2, f_2$.

The search for electric dipole radiative decays like $\phi \to a_0\gamma$, $f_0\gamma$ can clarify the structure of the lightest scalar mesons and help to determine whether or not are they mixed with four-quark states.

Accurate measurement of e^+e^- annihilation cross sections into hadrons is important for precision theoretical calculations of hadron contribution into muon anomalous magnetic moment (AMM). In the energy range $2E < 1$ GeV, the total hadron production cross section should be measured with the uncertainty of 0.5%. The corresponding error in AMM calculations would be 0.2 ppm.

The hadronic cross section is also of great importance to solve the problem of existence and location of light vector meson radial excitations ρ, ω, ϕ. This cross section also contributes significantly into some decay spectra and branching ratios of τ-lepton, D, and B mesons.

3.4 1995 Test Run[25]

The goal of the test run was to minimize background rate, adjust trigger components, and calibrate the calorimeter and drift chambers. At that time, the collider operated in the energy range 660–800 MeV with the CMD-2 detector, and the average luminosity was about $2 \times 10^{29}\ cm^{-2}sec^{-1}$. We installed lead shields around the beam pipe and found optimum trigger components, which allowed us to reduce the trigger rate to the level of $5 \times 10^4\ events \times nb$. The average event length on the tape was about 0.5 kByte. Using events of Bhabha scattering and two-photon annihilation, we measured the energy resolution of the SND calorimeter for 400 MeV electromagnetic showers to be 8% (σ), which should be compared with the MC value of 4%. Such a strong disagreement showed that the calorimeter calibration procedure was unsatisfactory at that time. The drift chamber system operated with a gas mixture $Ar + 10\% CO_2$. The spatial resolution measured using Bhabha events was about 0.2 mm in the r–ϕ plane, which was close to the expected value.

3.5 1996 ϕ(1020) Run

The energy range $2E = 984$–1034 MeV around the $\phi(1020)$ maximum was scanned with total integrated luminosity of 4 pb^{-1}. The number of produced ϕ's is estimated to be about 5×10^6. The VEPP-2M average luminosity was slightly above $10^{30}\ cm^{-2}sec^{-1}$. The normalized trigger rate was $10^7\ event \times pb$. After improvement of the energy calibration procedure, the calorimeter energy resolution reached $\sigma/E = 5.8\%$ for 500 MeV photons (Fig. 16), which is still larger than the expected value of 4.2%. The measured σ of the effective mass spectra of π^0, η, and K_s mesons, produced in the ϕ peak and decaying into photon final states, was 13, 18, and 26 MeV, respectively (Figs. 17, 18, 19).

Another important feature of SND is reconstruction of events with charged particles and photons together. For example, in the decay $\phi \to \eta\gamma \to \pi^+\pi^-\pi^0\gamma$, the reconstructed mass of η has the width of σ_{M_η}=20 MeV.

3.6 Preliminary Physical Results

In June 1996, about 10% of collected data corresponding to the integrated luminosity of 0.4 pb^{-1} was under processing. We selected the events of main $\phi(1020)$ decays like $\phi \to K^+K^-, K_sK_l, \eta\gamma$, etc. (Fig. 20). After the standard routine of

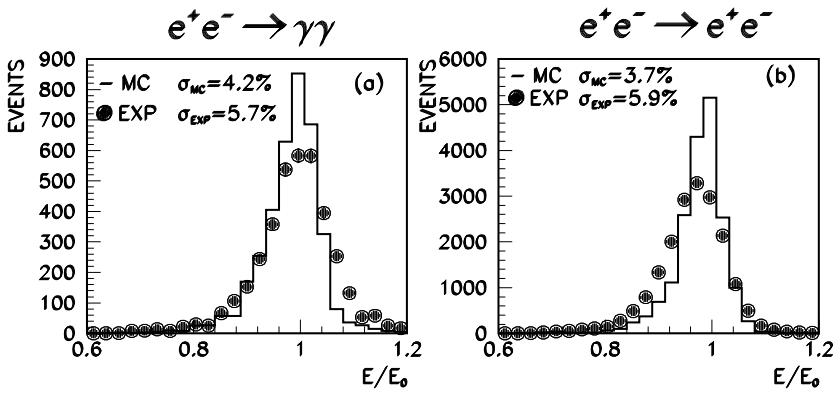

Figure 16: Energy spectra of electrons and photons for $e^+e^- \to e^+e^-$ and $e^+e^- \to \gamma\gamma$ reactions at $E_{beam} = 517\ MeV$.

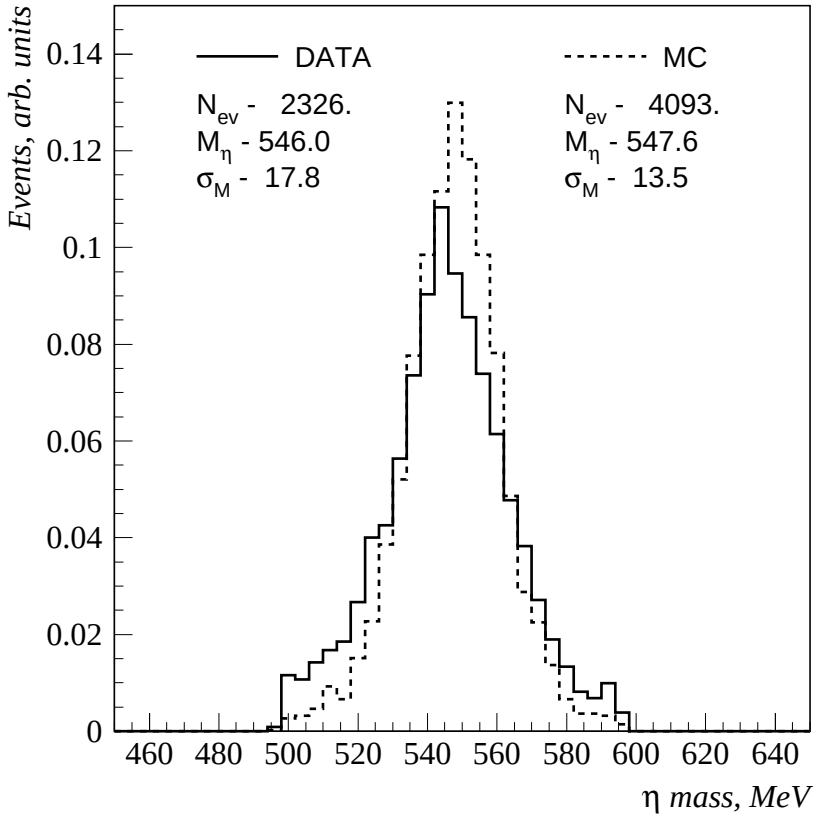

Figure 17: Effective mass spectrum of two photons for $e^+e^- \to \eta\gamma \to 3\gamma$ reaction.

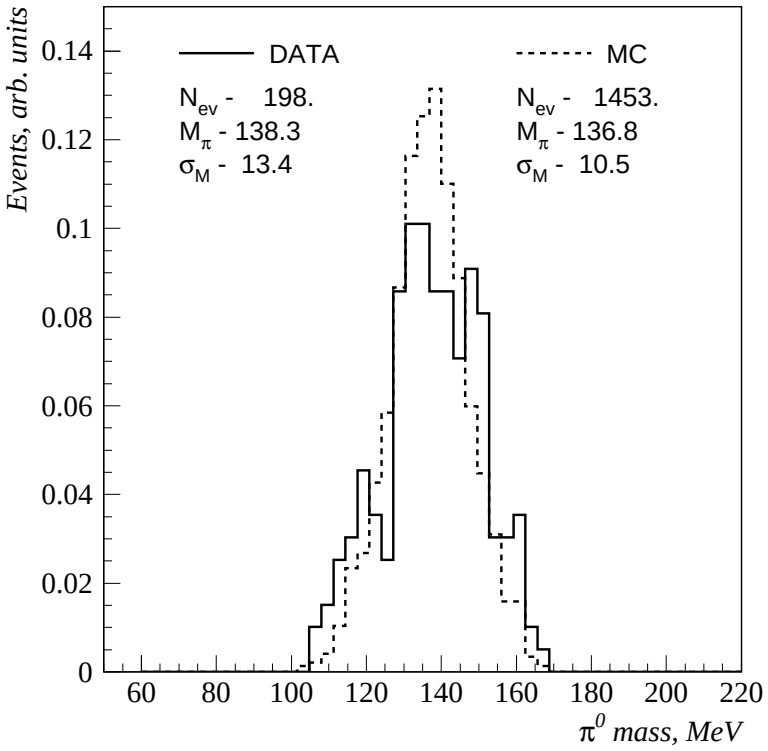

Figure 18: Effective mass spectrum of two photons for $e^+e^- \to \pi^0\gamma \to 3\gamma$ reaction.

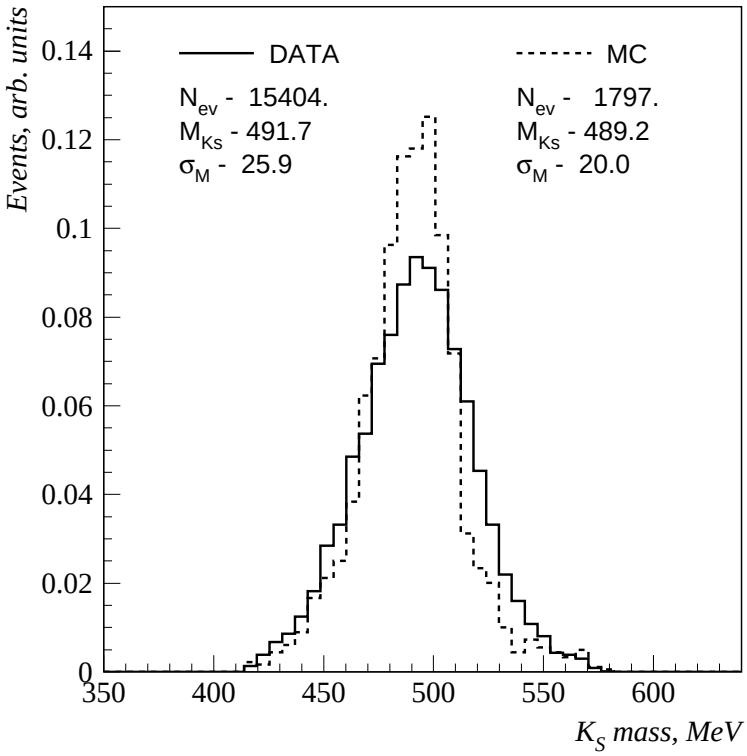

Figure 19: Effective mass spectrum of four photons for $Ks \to 2\pi^0$ decay.

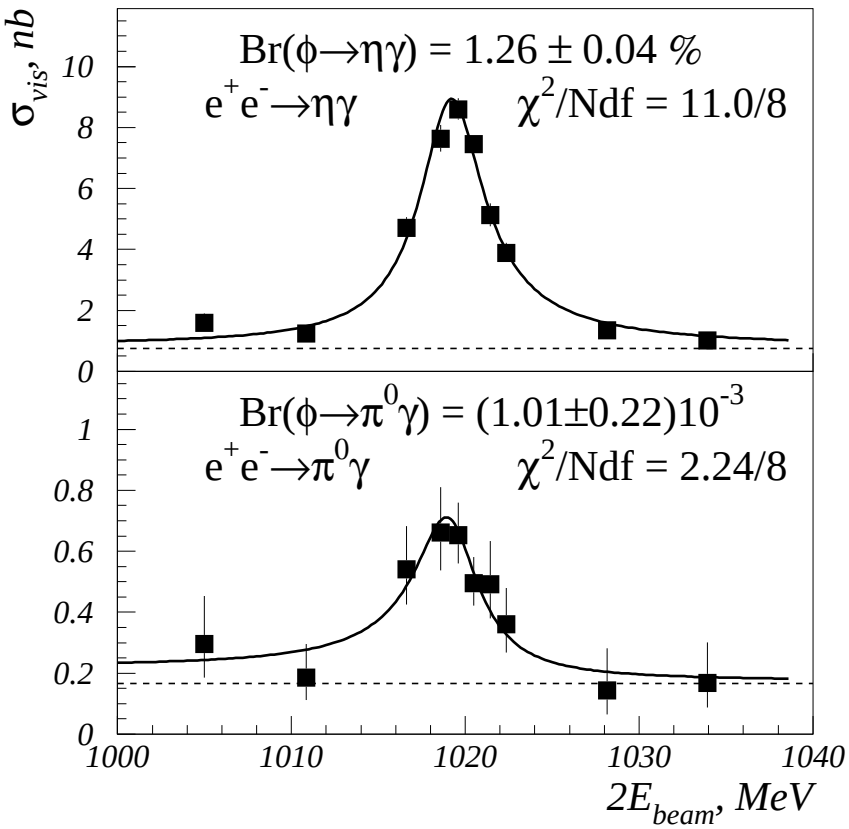

Figure 20: Visible cross section of $e^+e^- \to \eta\gamma$ and $e^+e^- \to \pi^0\gamma$ reactions.

fitting the obtained data with Breit-Wigner curve with radiative correction and applying the table data and MC efficiency for particular channels, we obtained the following preliminary data:

$B(\phi \to \eta\gamma) = (1.26 \pm 0.08)\%$ (from $\eta \to 2\gamma$ mode),

$B(\phi \to \eta\gamma) = (1.15 \pm 0.10)\%$ (from $\eta \to 3\pi^0$ mode),

$B(\phi \to \pi^0\gamma) = (0.10 \pm 0.02)\%$,

$B(\phi \to f_0(975)\gamma) < 9 \times 10^{-4}$ (from $f_0 \to 2\pi^0$ mode), (90% $C.L.$),

$B(\phi \to a_0(980)\gamma)B(a_0 \to \pi^0\eta) < 9 \times 10^{-4}$ (from $\eta \to 2\gamma$ mode), (90% $C.L.$).

The obtained data still have errors larger than in the tables and can be considered as a first step, showing the ability of SND to produce new physical results.

3.7 SND Summary

In Novosibirsk, experiments with the new SND detector at the low-energy collider VEPP-2M are continued. SND is a general-purpose nonmagnetic detector, the main part of which is the three-layer NaI(Tl) spherical calorimeter with 1632 individual crystals. SND provides a good possibility to study processes with multiple photons in final state. In summer 1996, the data-taking run in the vicinity of $\phi(1020)$ with the integrated luminosity of about 4 pb^{-1} was done. The measured photon energy resolution and mass resolution for π^0, η, K_s show feasibility of study of e^+e^- processes at VEPP-2M with SND. First preliminary physical results are obtained for $\phi(1020)$ decays.

Acknowledgments

This work is sponsored in part by the Soros Foundation, Grants No. RPX000 and RPX300, and the RFBR Fund, Grants No. 95-02-04587 and 96-02-19192.

References

References

[1] V. V. Anashin *et al.*, preprint Budker INP 84-114, Novosibirsk, 1984.

[2] L. M. Barkov *et al.*, *Nucl. Phys.* B **364**, 199 (1985).

[3] A. D. Bukin *et al.*, Sov. J. Nucl. Phys. **27**, 516 (1978).

[4] S. I. Dolinsky *et al.*, Phys. Report **202**, 99 (1991).

[5] G. A. Aksenov *et al.*, preprint Budker INP 85-118, Novosibirsk, 1985.

[6] E. V. Anashkin *et al.*, ICFA Instrumentation Bulletin 5 (1988), p.18.

[7] R. R. Akhmetshin *et al.*, *Phys. Lett.* B **364**, 199 (1995).

[8] R. R. Akhmetshin *et al.*, preprint Budker INP 95-62, Novosibirsk 1995.

[9] G. V. Fedotovich (CMD-2 Collaboration), in *Proceedings of the Workshop on Physics and Detectors for DAFNE'95*, Frascati, April 4-7, 1995, p. 571.

[10] L. Montanet *et al.*, *Phys. Rev.* D **54**, 341 (1996).

[11] N. N. Achasov, V. Gubin, and E. P. Solodov, hep-ph 9610282.

[12] A. Lysenko *et al.*, *Nucl. Instrum. Methods* A **359**, 419 (1995).

[13] V. N.Bayer, Russian ZETP **17**, 446 (1973).

[14] J. L. Rosner, I. Dunietz, and J. Hauser, *Phys. Rev.* D **35**, 2166 (1987).

[15] S. Eidelman, E. Solodov, and J. Thompson, *Nucl. Phys.* B **24**, 174 (1991).

[16] A. N. Skrinsky, in *Proceedings of the Workshop on Physics and Detectors for DAΦNE*, Frascati, April 1991, p. 67.

[17] G. Vignola, in *Proc. of the Workshop on Physics and Detectors for DAΦNE*, Frascati, April 1991, p. 11.

[18] A. N. Filippov *et al.*, in *Proceedings of the XVth Int. Conf. on High Energy Accelerators*, Hamburg, Germany, 1991, World Scientific, V. II, p. 1145.

[19] R. Baldini and A. Michetti, KLOE Memo 30, July 1995.

[20] G. Barbellini and C. Santoni, CERN-EP/89-8 and CERN-PPE/90-09.

[21] G. A. Sayer and E. F. Beall, *Phys. Rev.* D **169**, 1045 (1968).

[22] V. M. Aulchenko *et al.*, in *Proceedings of the Workshop on Physics and Detectors for DAΦNE*, Frascati, April 1991, p. 605; V. M. Aulchenko *et al.*, *The 6th International Conference on Hadron Spectroscopy*, Manchester, UK, 10–14 July 1995, p. 295.

[23] P. M. Beschastnov *et al.*, Nucl. Instrum. Methods A 342, 477 (1994).

[24] M. N. Achasov *et al.*, "Absolute energy calibration of the SND detector calorimeter by cosmic muons," to be published in *Proceedings of the VI International Conference on Instrumentation for Experiments at e^+e^- Colliders*, Novosibirsk, 1996.

[25] V. M. Aulchenko *et al.*, *Beginning of the Experiments with SND Detector at e^+e^- Collider VEPP-2M*, preprint Budker INP 95-56, 1995.